Alternative Theories of Dark Matter in the Light of Gravitational Lensing

Aysu Ece Saricaoglu

Washington University in St. Louis
Physics Department
a.saricaoglu@wustl.edu

October 23, 2025

Contents

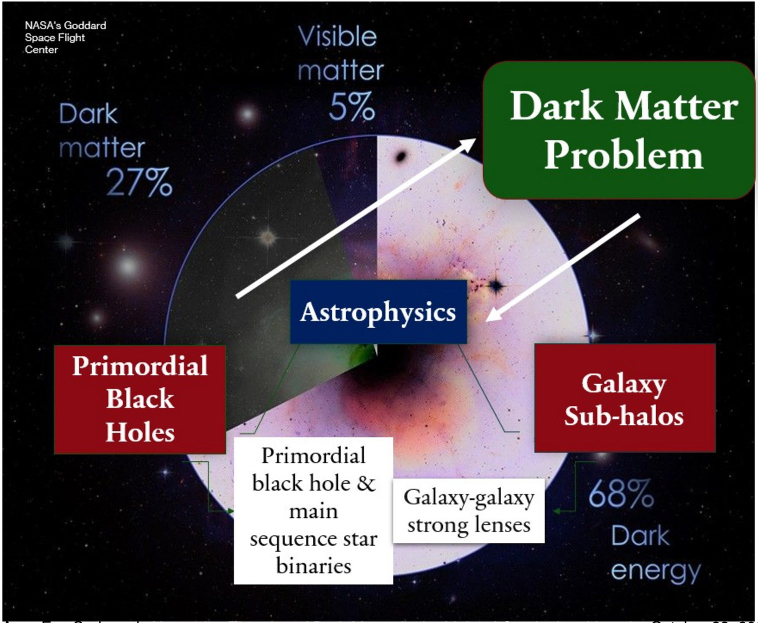

NASA's Goddard Space Flight Center
Visible matter 5%
Dark matter 27%
Dark Matter Problem
Astrophysics
Primordial Black Holes
Galaxy Sub-halos
Primordial black hole & main sequence star binaries
Galaxy-galaxy strong lenses
68% Dark energy

Part I: Star-Bound Primordial Black Holes as a Probe of Dark Matter

What are primordial black holes?

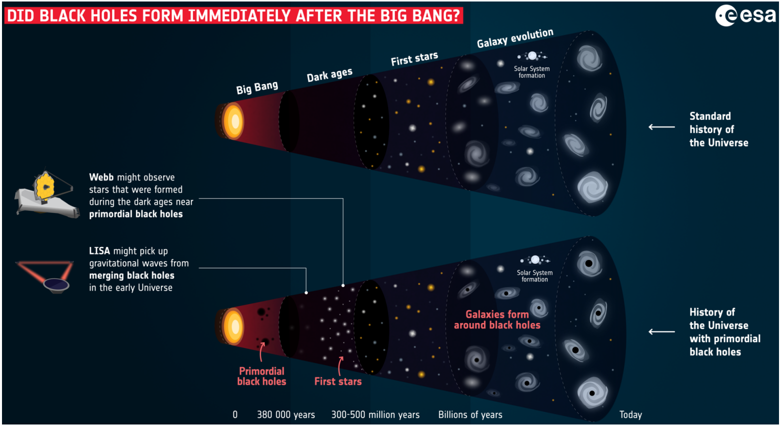

Image credits: European Space Agency (ESA)

PBHs as Cold Dark Matter Candidates

- Unless the limits from evaporation and CMB limits from Planck are relaxed the scenario of the dark matter fully composed of PBH is ruled out [11].
- The effect of various PBH fractions on the total power spectrum of the DM density field is shown in figure below compared to standard ΛCDM model [25].

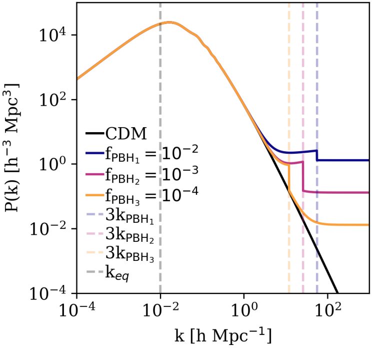

Adapted from Zhang, Bromm, and Liu [25] (Figure 1).

Why Black Hole - Main Sequence Star (BH-MS) Binaries?

- Primordial black holes in binary systems are detectable by their impact on the binary star light curves as a result of self-lensing.
- Initial work on compact object (CO) self-microlensing detectability consid ered MS star companions as unfavorable candidates compared to white dwarfs, since the source radius and the lens effect are inversely proportional [1].
- However, having more achievable photometry on brighter targets and a higher population to be monitored, Rahvar et al. [18] showed that MS stars are not less favorable targets than other CO.

Possible Scenarios for BH-MS Formation

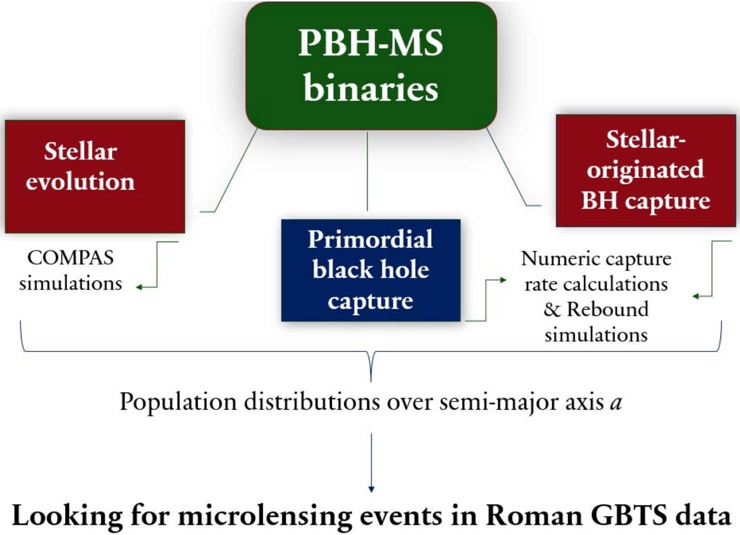

⇒ We need to be able to distinguish the scenarios of stellar binary evolution, dynamical capture of a stellar-originated BH, and capture of a PBH.
↪ In most cases, there is a degeneracy in the mass dimension of such systems.
⇒ However, the degeneracy on the semimajor axis for these three subpopulations of the BH-MS binaries might break.

I propose to use semimajor axis distributions to resolve the origins of the binary systems that will be detected by microlensing events.

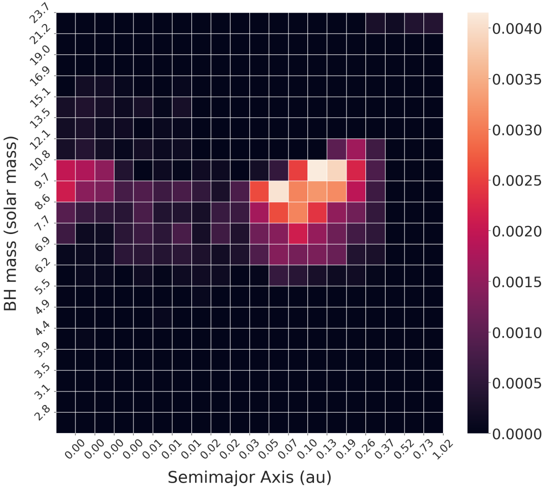

Occurence rate distribution over primary mass and semimajor axis for BH-MS binaries after their last MT event for $T < 70$ (days).

Binary Occurrences

We take the mean occurrence plots on Masuda & Hotokezaka's work [13] as a basis to compare with our simulation results.

Prospects of Finding Detached Black Hole–Star Binaries with *TESS*

Kento Masuda[1] and Kenta Hotokezaka

Department of Astrophysical Sciences, Princeton University, Princeton, NJ 08544, USA; kmasuda@astro.princeton.edu

Received 2018 August 31; revised 2019 August 1; accepted 2019 August 8; published 2019 October 1

Abstract

We discuss prospects of identifying and characterizing black hole (BH) companions to normal stars on tight but detached orbits, using photometric data from the *Transiting Exoplanet Survey Satellite* (*TESS*). We focus on the following two periodic signals from the visible stellar component: (i) in-eclipse brightening of the star due to gravitational microlensing by the BH (self-lensing), and (ii) a combination of ellipsoidal variations due to tidal distortion of the star and relativistic beaming due to its orbital motion (phase-curve variation). We evaluate the detectability of each signal in the light curves of stars in the *TESS* input catalog, based on a pre-launch noise model of *TESS* photometry as well as the actual light curves of spotted stars from the prime *Kepler* mission to gauge the potential impact of stellar activity arising from the tidally spun-up stellar components. We estimate that the self-lensing and phase-curve signals from BH companions, if they exist, will be detectable in the light curves of effectively $\mathcal{O}(10^5)$ and $\mathcal{O}(10^6)$ low-mass stars, respectively, taking into account orbital inclination dependence of the signals. These numbers could be large enough to actually detect signals from BHs: simple population models predict some 10 and 100 detectable BHs among these "searchable" stars; although, the latter may be associated with a comparable number of false positives due to stellar variabilities, and additional vetting with radial velocity measurements would be essential. Thus, the *TESS* data could serve as a resource to study nearby BHs with stellar companions on shorter-period orbits than will potentially be probed with *Gaia*.

Key words: stars: black holes – stars: neutron – techniques: photometric – white dwarfs

Residuals

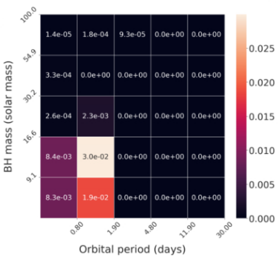

(a)

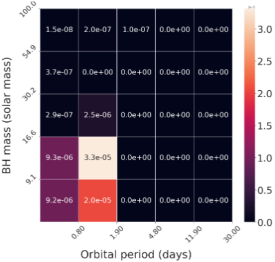

(b)

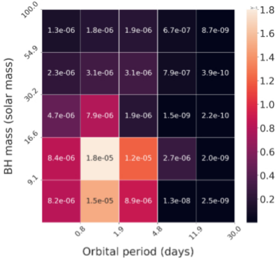

(c)

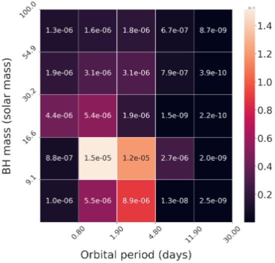

(d)

Residuals

⇒In Masuda & Hotokezaka [14], the 'searchability' constraint includes various criteria such as recovery rate as a function of the signal-to-noise ratio C_{rec} and the eclipse probability R_{star}/a

$$N_{eff} = \frac{R_{star}}{a} C_{rec}(\sqrt{n}\frac{s_{self-lensing}}{\sigma_{30min}}) \quad (1)$$

while the values compared above only include the criteria of edge-on configuration for the binaries, given by $cos_i \leq cos(89.9) \approx cos(\pi/2) = 0$

$$cos_i \leq cos(89.9) \approx cos(\pi/2) = 0 \quad (2)$$

which yields a *searchability index* of ≈ 0.0011.

Background

Among three mechanisms for the dynamical capture explained in detail by Lehmann et al. [12], in this work, I focus on two cases:

1. Losing energy to gravitational radiation due to rapid acceleration during single-body encounters, and becoming bound to the same object.
2. Losing mechanical energy to one object and becoming bound to another during a few-body encounter.

Capture cross section from gravitational radiation

Power radiated is given by the quadruple formula [7]

$$P = -\frac{G}{5c^2}\left\langle \frac{d^3 J_{ij}}{dt^3}\frac{d^3 J^{ij}}{dt^3}\right\rangle \tag{3}$$

$\rightarrow J_{ij}$:reduced quad. moment $\Rightarrow J_{ij} = I_{ij} - \frac{1}{3}\delta_{ij}\delta^{kl}I_{kl}$
$\rightarrow I_{ij}$:quad. moment tensor $\Rightarrow I(t)_{ij} = \int y^i y^j T^{00}(t,y)d^3y$

$$\Delta E_{GW} = \int_{-\infty}^{\infty} P(t)dt = \frac{8}{15}\frac{G^{7/2}}{c^5}\frac{M^{1/2}m_1^2 m_2^2}{r_{min}^{7/2}} g(e) \tag{4}$$

$$g(e) = \frac{\left[24\cos^{-1}\left(-\frac{1}{e}\right)\left(1+\frac{73}{24}e^2+\frac{37}{96}e^4\right)+(e^2-1)^{1/2}\left(\frac{301}{6}+\frac{673}{12}e^2\right)\right]}{(1+e)^{7/2}}$$

Capture cross section from gravitational radiation

$$r_{min} = \frac{GM}{v_\infty^2}(e-1) = \frac{GM_S}{v_\infty^2}\left(\sqrt{1+\frac{b^2 v_\infty^4}{G^2 M_S^2}} - 1\right) \tag{5}$$

Setting $r_{min} = R_S$ for R_S:radius of the star

$$b_{min} = \sqrt{R_S^2 + \frac{2GM_S R_S}{v_\infty^2}} \tag{6}$$

$b_{max} \rightarrow$ solved numerically.
$\Rightarrow$Capture condition:

$$\Delta E_{GW} > \frac{1}{2} M_{PBH} v_\infty^2$$

Capture cross section from gravitational radiation

Capture crossection by gravitational wave emission σ_{cap}^{GW} [12]

$$\sigma_{cap}^{GW} = \pi(b_{max} - b_{min})^2 \Theta(b_{max} - b_{min}) \tag{7}$$

hence the capture rate

$$R_{cap}^{GW} = n_\infty \langle \sigma_{cap} v_\infty \rangle = n_\infty \int dv f_\infty(v) \sigma_{cap} v \tag{8}$$

where

$$f_\infty(v) \propto v^2 exp(-\frac{v^2}{v_0^2}) \Theta(v_{esc} - v) \tag{9}$$

we take $v_0 = 220$km/s & $v_{esc} = 550$km/s

Capture cross section from gravitational radiation

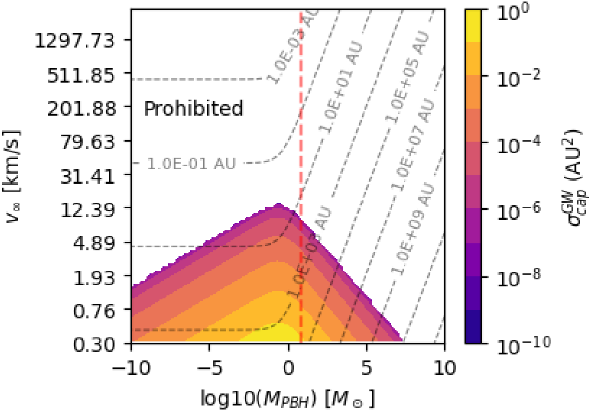

σ^{GW}_{cap} for GRO J0422 + 32 (V518 Per). Red dashes denote the mass of the black hole used in the calculations, $M_{BH} = 6.5\mathrm{M}_\odot$. Grey dashes show the semi-major axis values right after the capture.

For fixed v_∞,

$$\widetilde{N} = \widetilde{R_{cap}}/\widetilde{R_{ej}} \tag{10}$$

$$\langle \widetilde{N} \rangle = \int \frac{\widetilde{R}_{cap}}{\widetilde{R}_{ej}} = n_\infty \int d\mathbf{v}_\infty\, f(v_\infty)\, \frac{\widetilde{\sigma}_{cap}(v_\infty) v_1(v_\infty)}{\widetilde{R}_{ej}(v_\infty)} \tag{11}$$

where $\widetilde{\sigma}_{cap}$ is integrated over *da* & *de*
Also,

$$\widetilde{R}_{ej} \propto \eta(a,e), \quad \xi(a), \quad \kappa_\pm(\eta,\xi) \tag{12}$$

To obtain a closed-form estimate, we can use mean values instead of integrating over *da* & *de*

$$a :\to \bar{a}, \quad e :\to \bar{e}(\bar{a}) = \frac{1}{2}(1 + e_{min}) \tag{13}$$

Capture crossection from 3-body encounters

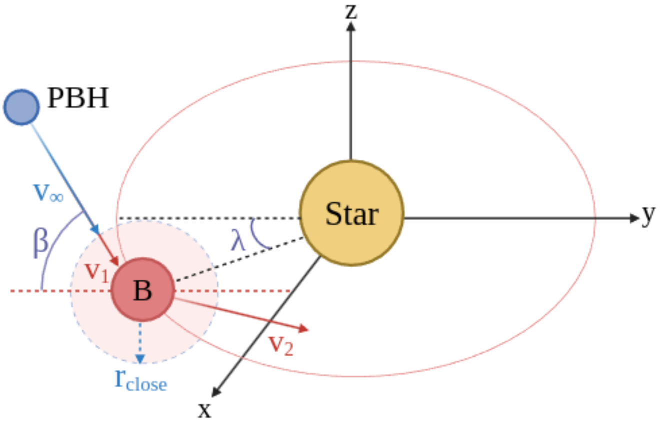

3-body encounter system of the main sequence star, celestial body B, and incident PBH. PBH with velocity v_∞ at infinity, has a close encounter with body B in the shaded region with initial velocity v_1 and exits the encounter with velocity v_2.

Case I | Example #1: Stable

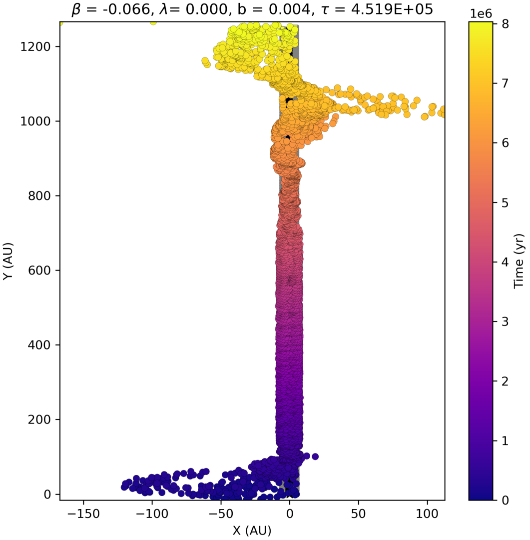

Case I | Example #1: Stable

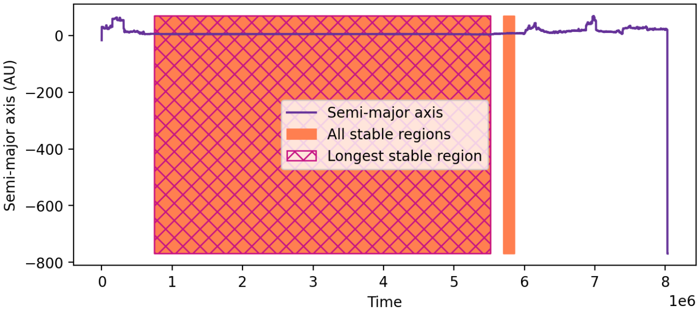

Case I | Example #2: Semi-stable

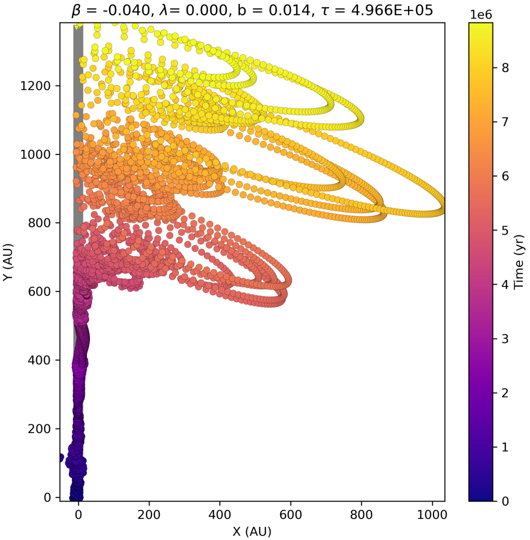

Case I | Example #2: Semi-stable

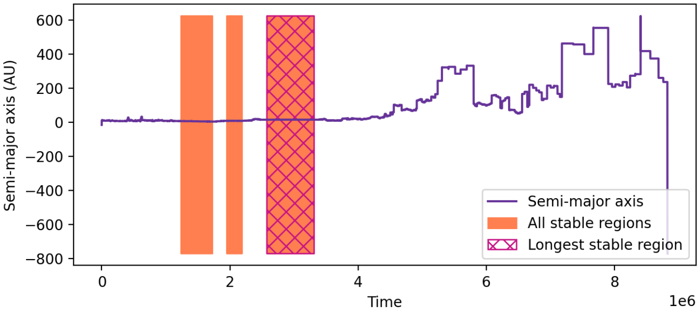

Case I | Example #3: Looks stable?

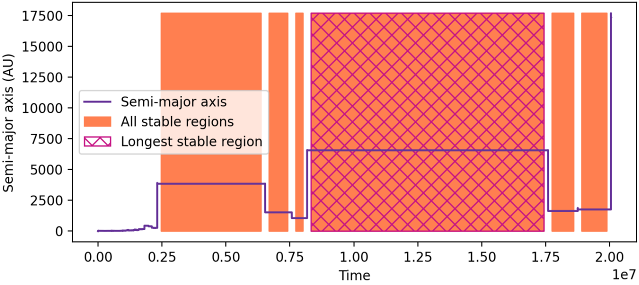

Case I | Example #3: Not so stable...

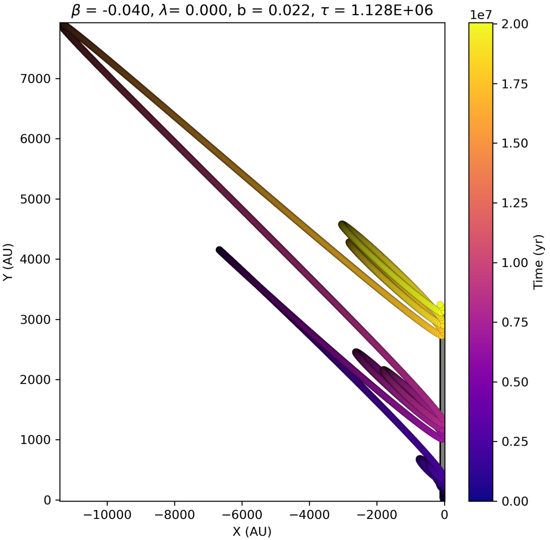

Case I | Initial Parameters

System	Sun-Jupiter system ($M_\odot$, M_J, a_{SJ})
Variables	$0 \leq \lambda \leq 2\pi$ $-\pi/2 \leq \beta \leq \pi/2$ $b_{\text{min}} \leq b \leq b_{\text{max}}$ AU
Fixed	$M_{\text{PBH}} = 10^{-13} M_\odot$, $v_\infty = 1.686$ AU/yr ≈ 7.999 km/s

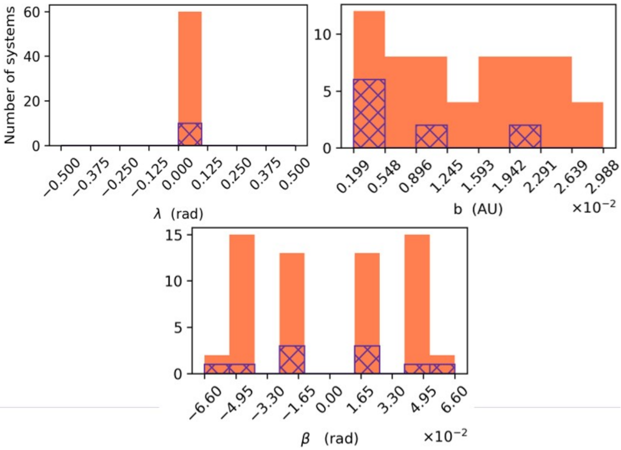

Case I | Population Yield

Captured Systems	60 sys. with $\tau_{\text{cap}} \geq 10^3\, T_{\text{Jupiter}} \approx 12000$ yr
Stable Orbits	10 sys. with ≥ 1000 yr cont. stability
Stable *a* Stats	$\langle \bar{a} \rangle = 4.897$ AU, $\langle a \rangle_d = 5.180$ AU

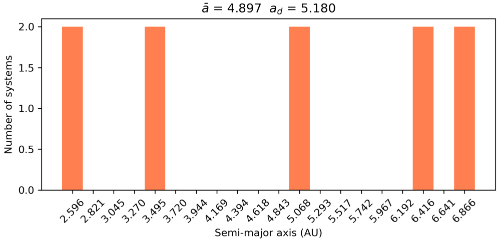

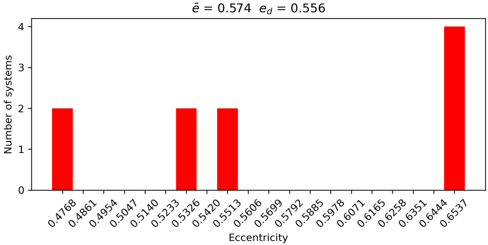

Case II | Initial Parameters

System	Sun-Jupiter system ($M_\odot$, M_J, a_{SJ})
Variables	$10^{-13} \leq M_{\rm PBH} \leq 10^{-4}$ $1 \leq v_\infty \leq 100$ km/s $b_{\rm min} \leq b \leq b_{\rm max}$ AU
Fixed	$\lambda = 0.0$, $\beta = 0.013$ rad

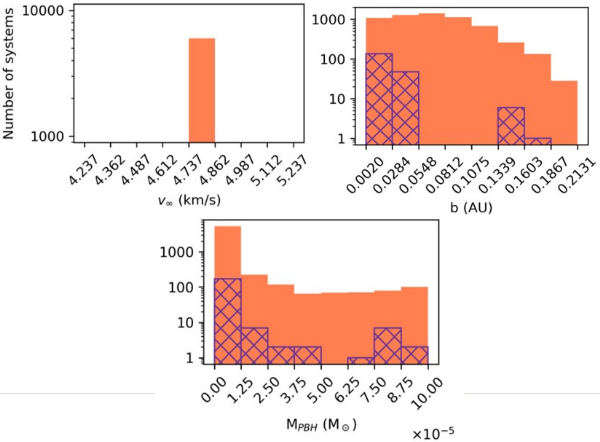

Case II | Population Yield

Captured Systems	6000 sys. $\tau_{\text{cap}} \geq 10^3\, T_{\text{Jupiter}} \approx 12000$ yr
Stable Orbits	192 sys. with ≥ 1000 yr cont. stability
Stable *a* Stats	$\langle \bar{a} \rangle = 5.438$ AU, $\langle a \rangle_d = 4.625$ AU

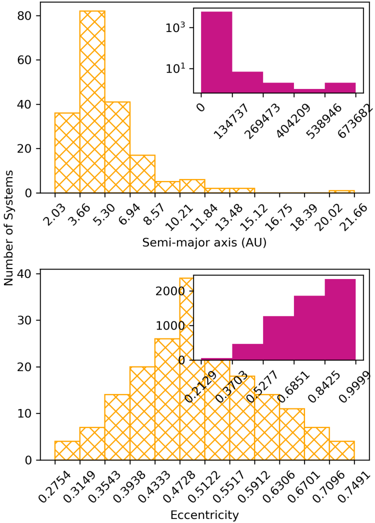

Case III | Initial Parameters

System	Sun-X System ($M_\odot$, M_X, a_{SX})
Variables	$10^{-3} \le M_X \le 10^{3.02}$ $\mathrm{M}_{Jupiter}$ $1 \le v_\infty \le 100$ km/s $0.0046 \le a \le 100$ AU
Fixed	$M_{\rm PBH} = 10^{-13} M_\odot$, $\lambda = 0.0$, $\beta = 0.013$ rad, b=$\bar{b}$

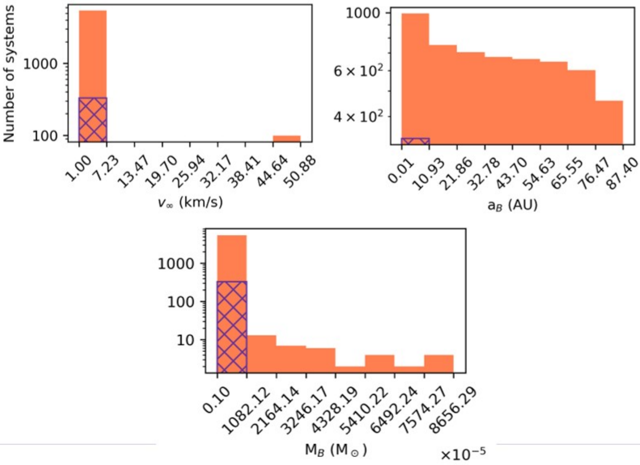

Case III | Population Yield

Captured Systems	5496 sys. $\tau_{\text{cap}} \geq 10^3\,T_{\text{Jupiter}} \approx 12000$ yr
Stable Orbits	329 sys. with ≥ 1000 yr cont. stability
Stable *a* Stats	$\langle \bar{a} \rangle = 36.299$ AU, $\langle a \rangle_d = 27.112$ AU

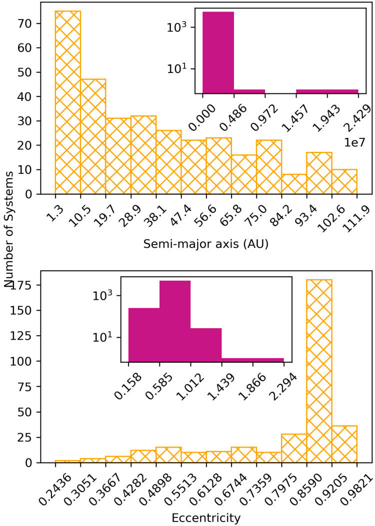

About what we proposed...

From evolution simulation and the capture calculations we roughly see that binaries evolved together undergoing mass transfer events have $a < 1$ AU while those formed by capture have $a > 1$ AU.
For ≤ 120 AU, $a_{\text{min}} = 2.48$ from the first case, $a_{\text{min}} = 1.65$ AU from the second case, for stable durations

Preliminary conclusions

1. v_{inf} of stellar BHs kicked out of their binaries and free floating PBH might be different, directly affecting the capture rates with any methods
2. For now, capture rate calculations from GW can be used to test the possibility of forming by capture of an observed system. In my future work, I will eventually derive the capture rates.

What's Next?

- Evaluation $\langle \bar{N} \rangle$ from the three-body capture and ejection crossections calculated so far
- More simulations on a larger variety of initial parameters, better analysis of the relation between the parameters that enable capture events and their occurrence in nature.
- Create a simulation and analysis pipeline development towards searching microlensing signals in the upcoming Roman data.

Part II: Galaxy-Scale Strong Lenses as a Probe of Dark Matter

Background

- In ΛCDM, gravity is the source that is responsible for the structure formation by hierarchical merging of smaller structures. Such structures are held in the gravitational potential well of the massive halo and referred to as sub-halos.

Subhalo Structure - Simulations

⇒ For ΛCDM, various studies by Navarro et al. utilizing N-body simulations led to a 'universal' density profile, known as **The Navarro–Frenk–White (NFW) profile** :

$$\frac{\rho(r)}{\rho_{crit}} = \frac{\delta_c}{\frac{r}{r_s}(1 + \frac{r}{r_s})^2} \tag{14}$$

where r_s is the characteristic radius of the halo (scale radius), δ_c is the characteristic density and $\rho_{crit} = 3H^2/8\pi G$ is the critical density [17, 16].

$\Rightarrow$ The rotation curves inferred from the observations of the dark matter-dominated Low-Surface-Brightness(LSB) galaxies sides with the 'pseudo-isothermal' (PI) sphere profile,

$$\rho_{PI} = \frac{\rho_0}{1 + (\frac{r}{R_C})^2} \tag{15}$$

where R_C is the core radius of the halo [17, 2].

Core-Cusp Problem

If $\rho \sim r^{\alpha}$, as r $\to$ 0;

- The NFW density profile given by the simulations yields a slope with $\alpha = -1 \Leftrightarrow$ a *cusp*!
- The PI density profile inferred by the observed rotation curves indicates a constant density region with $\alpha = 0 \Leftrightarrow$ a *core*!

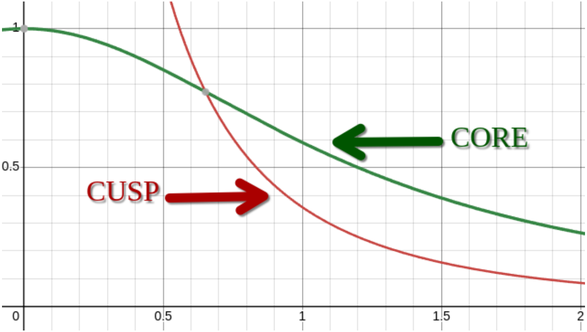

⟶ *The small scale crisis in cosmology*

The discrepancy between the density profiles given by observations and simulations is known as the *core-cusp problem* [2].

- Possible solutions include warm dark matter (WDM) and self-interacting dark matter (SIDM) models as alternatives for the ΛCDM [8].
- SIDM predicts that the dark matter halos might undergo gravothermal collapse, resulting in a steep density profile formation and increased overall central halo density. In such a scenario, individual galaxies in clusters would act as strong lenses and produce arcseconds scale multiple images [23, 15].

Galaxy Scale Strong Lenses (GSSL)

- Hence, GSSLs formed by massive elliptical galaxies and dwarf galaxies are expected to provide insights into the problem.
- Luckily, The Large Synoptic Survey Telescope (LSST) at the Rubin Observatory is expected to make an impactful contribution to the GSSL population from both galaxy types [21].
- At this part of my work, I will focus on the GSSL analysis in the upcoming LSST data, including possible effects of the contaminated exposures.

LSST Simulations on Lenstronomy

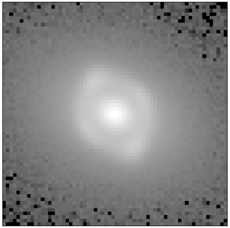

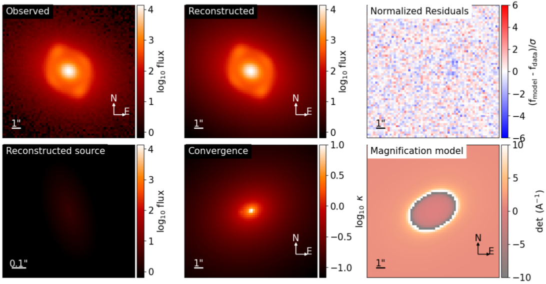

GSSL simulated for LSST, g-band.

What's Next?

- Repeat the analysis procedure on the HSC data using LSST pipelines, determine R_C detection sensitivity with LSST.
- Include LSST observation simulations (ObSim) on the pipeline to prepare for detection and analysis of the GSSL on the upcoming LSST data.

Thank you for listening!

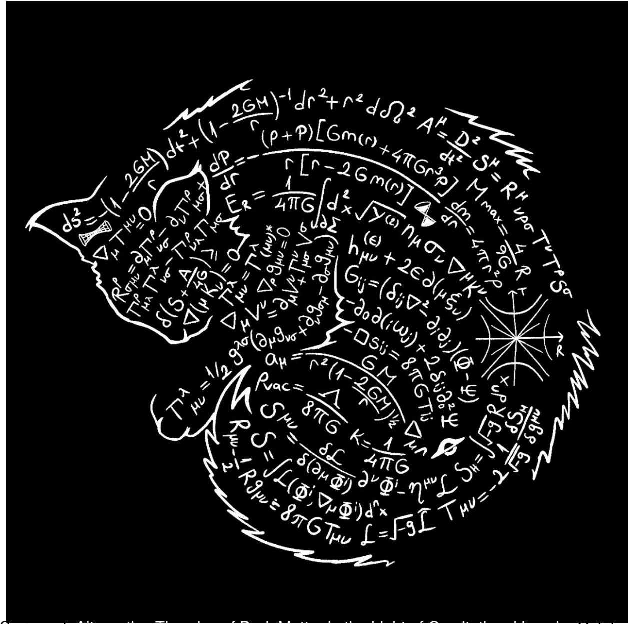

References I

[1] G. M. Beskin and A. V. Tuntsov. "Detection of compact objects by means of gravitational lensing in binary systems". en. In: *Astronomy & Astrophysics* 394.2 (Nov. 2002). Number: 2 Publisher: EDP Sciences, pp. 489–503. ISSN: 0004-6361, 1432-0746. DOI: 10.1051/0004-6361:20021150. URL: https://www.aanda.org/articles/aa/abs/2002/41/aa2132/aa2132.html (visited on 01/21/2025).

[2] W. J. G. de Blok. "The Core-Cusp Problem". en. In: *Advances in Astronomy* 2010.1 (2010). _eprint: https://onlinelibrary.wiley.com/doi/pdf/10.1155/2010/789293, p. 789293. ISSN: 1687-7977. DOI: 10.1155/2010/789293. URL: https://onlinelibrary.wiley.com/doi/abs/10.1155/2010/789293 (visited on 03/10/2025).

[3] B. J. Carr and James E. Lidsey. "Primordial black holes and generalized constraints on chaotic inflation". In: *Physical Review D* 48.2 (July 1993). Publisher: American Physical Society, pp. 543–553. DOI: 10.1103/PhysRevD.48.543. URL: https://link.aps.org/doi/10.1103/PhysRevD.48.543 (visited on 01/20/2025).

[4] Bernard Carr and Florian Kühnel. "Primordial black holes as dark matter candidates". en. In: *SciPost Physics Lecture Notes* (May 2022), p. 048. ISSN: 2590-1990. DOI: 10.21468/SciPostPhysLectNotes.48. URL: https://scipost.org/10.21468/SciPostPhysLectNotes.48 (visited on 01/20/2025).

[5] Bernard Carr and Florian Kühnel. "Primordial Black Holes as Dark Matter: Recent Developments". In: *Annual Review of Nuclear and Particle Science* 70.1 (Oct. 2020), pp. 355–394. ISSN: 1545-4134. DOI: 10.1146/annurev-nucl-050520-125911. URL: http://dx.doi.org/10.1146/annurev-nucl-050520-125911.

[6] Bernard Carr et al. "Constraints on primordial black holes". In: *Reports on Progress in Physics* 84 (Nov. 2021). Publisher: IOP ADS Bibcode: 2021RPPh...84k6902C, p. 116902. ISSN: 0034-4885. DOI: 10.1088/1361-6633/ac1e31. URL: https://ui.adsabs.harvard.edu/abs/2021RPPh...84k6902C (visited on 02/24/2025).

[7] Sean M. Carroll. *Spacetime and Geometry: An Introduction to General Relativity*. en. ISBN: 9781108770385 Publisher: Cambridge University Press. Aug. 2019. DOI: 10.1017/9781108770385. URL: https://www.cambridge.org/highereducation/books/spacetime-and-geometry/38EDABF9E2BADCE6FBCF2B22DC12BFFE (visited on 04/22/2025).

[8] Oliver D. Elbert et al. "Core formation in dwarf haloes with self-interacting dark matter: no fine-tuning necessary". In: *Monthly Notices of the Royal Astronomical Society* 453.1 (Oct. 2015), pp. 29–37. ISSN: 0035-8711. DOI: 10.1093/mnras/stv1470. URL: https://doi.org/10.1093/mnras/stv1470 (visited on 03/10/2025).

[9] Stephen Hawking. "Gravitationally Collapsed Objects of Very Low Mass". In: *Monthly Notices of the Royal Astronomical Society* 152.1 (Apr. 1971), pp. 75–78. ISSN: 0035-8711. DOI: 10.1093/mnras/152.1.75. eprint: https://academic.oup.com/mnras/article-pdf/152/1/75/9360899/mnras152-0075.pdf. URL: https://doi.org/10.1093/mnras/152.1.75.

[10] P. Ivanov, P. Naselsky, and I. Novikov. "Inflation and primordial black holes as dark matter". In: *Physical Review D* 50.12 (Dec. 1994). Publisher: American Physical Society, pp. 7173–7178. DOI: 10.1103/PhysRevD.50.7173. URL: https://link.aps.org/doi/10.1103/PhysRevD.50.7173 (visited on 01/20/2025).

[11] Benjamin V. Lehmann, Stefano Profumo, and Jackson Yant. "The maximal-density mass function for primordial black hole dark matter". en. In: *Journal of Cosmology and Astroparticle Physics* 2018.04 (Apr. 2018), p. 007. ISSN: 1475-7516. DOI: 10.1088/1475-7516/2018/04/007. URL: https://dx.doi.org/10.1088/1475-7516/2018/04/007 (visited on 02/24/2025).

[12] Benjamin V. Lehmann et al. "Capture of primordial black holes in extrasolar systems". en. In: *Journal of Cosmology and Astroparticle Physics* 2022.08 (Aug. 2022), p. 079. ISSN: 1475-7516. DOI: 10.1088/1475-7516/2022/08/079. URL: https://iopscience.iop.org/article/10.1088/1475-7516/2022/08/079 (visited on 12/30/2024).

References III

[13] Kento Masuda and Kenta Hotokezaka. "Prospects of Finding Detached Black Hole-Star Binaries with TESS". In: *The Astrophysical Journal* 883.2 (Oct. 2019). arXiv:1808.10856 [astro-ph], p. 169. ISSN: 0004-637X, 1538-4357. DOI: 10.3847/1538-4357/ab3a4f. URL: http://arxiv.org/abs/1808.10856 (visited on 01/18/2025).

[14] Kento Masuda and Kenta Hotokezaka. "Prospects of Finding Detached Black Hole-Star Binaries with TESS". In: *The Astrophysical Journal* 883.2 (Oct. 2019). arXiv:1808.10856 [astro-ph], p. 169. ISSN: 0004-637X, 1538-4357. DOI: 10.3847/1538-4357/ab3a4f. URL: http://arxiv.org/abs/1808.10856 (visited on 01/18/2025).

[15] P. Natarajan et al. "Strong Lensing by Galaxy Clusters". en. In: *Space Science Reviews* 220.2 (Feb. 2024), p. 19. ISSN: 1572-9672. DOI: 10.1007/s11214-024-01051-8. URL: https://doi.org/10.1007/s11214-024-01051-8 (visited on 03/10/2025).

[16] Julio F. Navarro, Carlos S. Frenk, and Simon D. M. White. "A Universal Density Profile from Hierarchical Clustering". en. In: *The Astrophysical Journal* 490.2 (Dec. 1997). Publisher: IOP Publishing, p. 493. ISSN: 0004-637X. DOI: 10.1086/304888. URL: https://iopscience.iop.org/article/10.1086/304888/meta (visited on 03/20/2025).

[17] Julio F. Navarro, Carlos S. Frenk, and Simon D. M. White. "The Structure of Cold Dark Matter Halos". In: *The Astrophysical Journal* 462 (May 1996). Publisher: IOP ADS Bibcode: 1996ApJ...462..563N, p. 563. ISSN: 0004-637X. DOI: 10.1086/177173. URL: https://ui.adsabs.harvard.edu/abs/1996ApJ...462..563N (visited on 03/20/2025).

[18] S. Rahvar, A. Mehrabi, and M. Dominik. "Compact object detection in self-lensing binary systems with a main-sequence star". In: *Monthly Notices of the Royal Astronomical Society* 410.2 (Jan. 2011), pp. 912–918. ISSN: 0035-8711. DOI: 10.1111/j.1365-2966.2010.17490.x. URL: https://doi.org/10.1111/j.1365-2966.2010.17490.x (visited on 01/20/2025).

[19] Jeff Riley et al. "Rapid Stellar and Binary Population Synthesis with COMPAS". In: *The Astrophysical Journal Supplement Series* 258 (Feb. 2022). Publisher: IOP ADS Bibcode: 2022ApJS..258...34R, p. 34. ISSN: 0067-0049. DOI: 10.3847/1538-4365/ac416c. URL: https://ui.adsabs.harvard.edu/abs/2022ApJS..258...34R (visited on 02/04/2025).

[20] Misao Sasaki et al. "Primordial black holes—perspectives in gravitational wave astronomy". In: *Classical and Quantum Gravity* 35.6 (Feb. 2018), p. 063001. DOI: 10.1088/1361-6382/aaa7b4. URL: https://dx.doi.org/10.1088/1361-6382/aaa7b4.

[21] Anowar J. Shajib et al. *Strong gravitational lenses from the Vera C. Rubin Observatory*. arXiv:2406.08919 [astro-ph]. Feb. 2025. DOI: 10.48550/arXiv.2406.08919. URL: http://arxiv.org/abs/2406.08919 (visited on 03/10/2025).

[22] Pablo Villanueva-Domingo, Olga Mena, and Sergio Palomares-Ruiz. "A Brief Review on Primordial Black Holes as Dark Matter". en. In: *Frontiers in Astronomy and Space Sciences* 8 (May 2021), p. 681084. ISSN: 2296-987X. DOI: 10.3389/fspas.2021.681084. URL: https://www.frontiersin.org/articles/10.3389/fspas.2021.681084/full (visited on 12/30/2024).

[23] Daneng Yang and Hai-Bo Yu. "Self-interacting dark matter and small-scale gravitational lenses in galaxy clusters". In: *Physical Review D* 104.10 (Nov. 2021). Publisher: American Physical Society, p. 103031. DOI: 10.1103/PhysRevD.104.103031. URL: https://link.aps.org/doi/10.1103/PhysRevD.104.103031 (visited on 03/20/2025).

[24] Ya. B. Zel'dovich and I. D. Novikov. "The Hypothesis of Cores Retarded during Expansion and the Hot Cosmological Model". In: 43 (Jan. 1966), p. 758.

[25] Saiyang Zhang, Volker Bromm, and Boyuan Liu. "How Do Primordial Black Holes Change the Halo Mass Function and Structure?" en. In: *The Astrophysical Journal* 975.1 (Oct. 2024). Publisher: The American Astronomical Society, p. 139. ISSN: 0004-637X. DOI: 10.3847/1538-4357/ad7b0d. URL: https://dx.doi.org/10.3847/1538-4357/ad7b0d (visited on 02/24/2025).

What are primordial black holes?

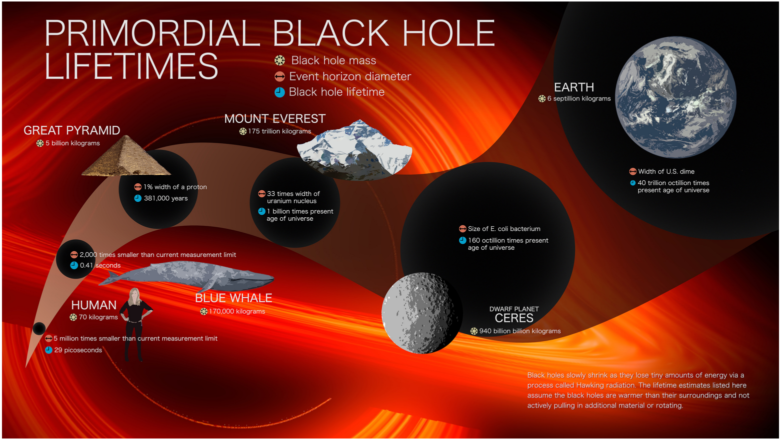

What are primordial black holes?

- Primordial black holes (PBHs) are hypothetical objects that could have formed as highly over-dense regions collapse gravitationally in the early universe, by mechanisms such as adiabatic quantum fluctuations appearing during inflation [3, 10], collapse from density fluctuations and various collapse scenarios including domain walls, cosmic loops, bubble collisions [4].
- They have non-stellar origins [20].
- First suggested in [24], and also independently in [9], they have been a source of attention for almost 50 years due to their extraordinary properties such as constituting primordial non-baryonic matter from the radiation-dominated era [22, 5]

Mass Models

- They can be small enough to get affected by the Hawking radiation, smaller than 10^{15}g.[**kuhler**]
- Therefore it is wiser to inspect primordial black holes (PBHs) more massive than that.
- For PHBs to be accounted for the cold dark matter, they should be in one of these mass windows [**kuhler**]:
  $\longrightarrow$ the asteroid mass range($10^{16} - 10^{17}$g)
  $\longrightarrow$ the sublunar mass range ($10^{20} - 10^{26}$g)
  $\longrightarrow$ the intermediate mass range (10-10^3 M_{sun})
- Even if they fall into one of these windows, they may not provide *all* dark matter [**kuhler**].

DISCLAIMER

Mass Models

From Carr et al., 2021 [6]

other cosmological conundra. In particular, many authors have discussed the possibility that PBHs could provide the dark matter [22, 562]. In this context, Fig. 10 might suggest that the asteroid range $10^{17}\,\mathrm{g} < M < 10^{23}\,\mathrm{g}$ between the EGB and HSC microlensing limits is most plausible. However, the intermediate range $10\,M_\odot < M < 10^2\,M_\odot$ between the LMC microlensing and wide binary limits is still favored by some theorists, even though this appears to violate other constraints, because PBHs may naturally form in this range. In principle, Fig. 10 suggests that a lot of dark matter could reside in "stupendously large black holes" in the range $10^{14}\,M_\odot < M < 10^{17}\,M_\odot$, although the lack of constraints there probably just reflects the fact that little attention has been paid to this possibility and obviously such SLABs could not provide dark matter inside galactic halos [426]. A final possibility is the Planck-mass relics of Hawking evaporation in the range around $M \sim 10^{-5}\,\mathrm{g}$, although this is probably untestable unless the relics are electrically charged [138].

Primordial black holes as dark matter candidates

Bernard Carr[1*] and Florian Kühnel[2†]

1 School of Physics and Astronomy, Queen Mary University of London,
Mile End Road, London E1 4NS, United Kingdom
2 Arnold Sommerfeld Center, Ludwig-Maximilians-Universität,
Theresienstraße 37, 80333 München, Germany

⋆ b.j.carr@qmul.ac.uk, † florian.kuehnel@physik.uni-muenchen.de

This article is partly based on our recent review [1], where more details of topics covered can be found.

ÉCOLE DE PHYSIQUE DES HOUCHES

Part of the Dark Matter
Session 118 of the Les Houches School, July 2021
published in the Les Houches Lecture Notes Series

Abstract

We review the formation and evaporation of primordial black holes (PBHs) and their possible contribution to dark matter. Various constraints suggest they could only provide most of it in the mass windows 10^{17} – 10^{23} g or 10 – 10^2 $M_\odot$, with the last possibility perhaps being suggested by the LIGO/Virgo observations. However, PBHs could have important consequences even if they have a low cosmological density. Sufficiently large ones might generate cosmic structures and provide seeds for the supermassive black holes in galactic nuclei. Planck-mass relics of PBH evaporations or stupendously large black holes bigger than 10^{12} $M_\odot$ could also be an interesting dark component.

Why Black Hole - Main Sequence Star (BH-MS) Binaries?

- Primordial black holes in binary systems are detectable by their impact on the binary star light curves as a result of self-lensing.
- Initial work on compact object (CO) self-microlensing detectability considered MS star companions as unfavorable candidates compared to white dwarfs, since the source radius and the lens effect are inversely proportional [1].
- However, having more achievable photometry on brighter targets and a higher population to be monitored, Rahvar et al. [18] showed that MS stars are not less favorable targets than other CO.

Stellar Evolution Binary System Distributions via COMPAS

- I use the rapid stellar and binary population synthesis tool COMPAS to simulate parameter distribution and occurrence of BH-MS systems in nature [19].

Binary Occurrences

We take the mean occurrence plots on Masuda & Hotokezaka's work [13] as a basis to reproduce them using COMPAS results.

Prospects of Finding Detached Black Hole–Star Binaries with *TESS*

Kento Masuda[1] and Kenta Hotokezaka
Department of Astrophysical Sciences, Princeton University, Princeton, NJ 08544, USA; kmasuda@astro.princeton.edu
Received 2018 August 31; revised 2019 August 1; accepted 2019 August 8; published 2019 October 1

Abstract

We discuss prospects of identifying and characterizing black hole (BH) companions to normal stars on tight but detached orbits, using photometric data from the *Transiting Exoplanet Survey Satellite* (*TESS*). We focus on the following two periodic signals from the visible stellar component: (i) in-eclipse brightening of the star due to gravitational microlensing by the BH (self-lensing), and (ii) a combination of ellipsoidal variations due to tidal distortion of the star and relativistic beaming due to its orbital motion (phase-curve variation). We evaluate the detectability of each signal in the light curves of stars in the *TESS* input catalog, based on a pre-launch noise model of *TESS* photometry as well as the actual light curves of spotted stars from the prime *Kepler* mission to gauge the potential impact of stellar activity arising from the tidally spun-up stellar components. We estimate that the self-lensing and phase-curve signals from BH companions, if they exist, will be detectable in the light curves of effectively $\mathcal{O}(10^5)$ and $\mathcal{O}(10^6)$ low-mass stars, respectively, taking into account orbital inclination dependence of the signals. These numbers could be large enough to actually detect signals from BHs: simple population models predict some 10 and 100 detectable BHs among these "searchable" stars; although, the latter may be associated with a comparable number of false positives due to stellar variabilities, and additional vetting with radial velocity measurements would be essential. Thus, the *TESS* data could serve as a resource to study nearby BHs with stellar companions on shorter-period orbits than will potentially be probed with *Gaia*.

Key words: stars: black holes – stars: neutron – techniques: photometric – white dwarfs

Residuals

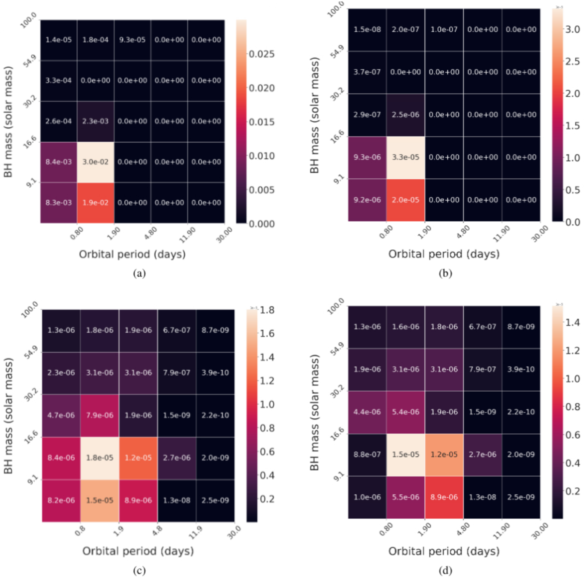
BH mass (solar mass)
100.0
54.9
30.2
16.6
9.1
1.4e-05 1.8e-04 9.3e-05 0.0e+00 0.0e+00
3.3e-04 0.0e+00 0.0e+00 0.0e+00 0.0e+00
2.6e-04 2.3e-03 0.0e+00 0.0e+00 0.0e+00
8.4e-03 3.0e-02 0.0e+00 0.0e+00 0.0e+00
8.3e-03 1.9e-02 0.0e+00 0.0e+00 0.0e+00
0.025
0.020
0.015
0.010
0.005
0.000
0.80
1.90
4.80
11.90
30.00
Orbital period (days)
(a)
BH mass (solar mass)
100.0
54.9
30.2
16.6
9.1
1.5e-08 2.0e-07 1.0e-07 0.0e+00 0.0e+00
3.7e-07 0.0e+00 0.0e+00 0.0e+00 0.0e+00
2.9e-07 2.5e-06 0.0e+00 0.0e+00 0.0e+00
9.3e-06 3.3e-05 0.0e+00 0.0e+00 0.0e+00
9.2e-06 2.0e-05 0.0e+00 0.0e+00 0.0e+00
3.0
2.5
2.0
1.5
1.0
0.5
0.0
0.80
1.90
4.80
11.90
30.00
Orbital period (days)
(b)
BH mass (solar mass)
100.0
54.9
30.2
16.6
9.1
1.3e-06 1.8e-06 1.9e-06 6.7e-07 8.7e-09
2.3e-06 3.1e-06 3.1e-06 7.9e-07 3.9e-10
4.7e-06 7.9e-06 1.9e-06 1.5e-09 2.2e-10
8.4e-06 1.8e-05 1.2e-05 2.7e-06 2.0e-09
8.2e-06 1.5e-05 8.9e-06 1.3e-08 2.5e-09
1.8
1.6
1.4
1.2
1.0
0.8
0.6
0.4
0.2
0.8
1.9
4.8
11.9
30.0
Orbital period (days)
(c)
BH mass (solar mass)
100.0
54.9
30.2
16.6
9.1
1.3e-06 1.6e-06 1.8e-06 6.7e-07 8.7e-09
1.9e-06 3.1e-06 3.1e-06 7.9e-07 3.9e-10
4.4e-06 5.4e-06 1.9e-06 1.5e-09 2.2e-10
8.8e-07 1.5e-05 1.2e-05 2.7e-06 2.0e-09
1.0e-06 5.5e-06 8.9e-06 1.3e-08 2.5e-09
1.4
1.2
1.0
0.8
0.6
0.4
0.2
0.80
1.90
4.80
11.90
30.00
Orbital period (days)
(d)

Residuals

⇒In Masuda & Hotokezaka [14], the 'searchability' constraint includes various criteria such as recovery rate as a function of the signal-to-noise ratio C_{rec} and the eclipse probability R_{star}/a

$$N_{eff} = \frac{R_{star}}{a} C_{rec}(\sqrt{n}\frac{s_{self-lensing}}{\sigma_{30min}}) \tag{16}$$

while the values compared above only include the criteria of edge-on configuration for the binaries, given by $cos_i \leq cos(89.9) \approx cos(\pi/2) = 0$

$$cos_i \leq cos(89.9) \approx cos(\pi/2) = 0 \tag{17}$$

which yields a *searchability index* of ≈ 0.0011.

Statistics Summary

Table 1: Updated quantities from the simulation log file.

Quantity	Pre-MT	Post-MT	Post Last MT
Number of systems	29,000,000	-	-
Number of systems forming MT (via SP STATUS)	17,029,983	-	-
Number of primary mass BHs	2,207,804	2,671,970	-
Number of secondary mass BHs	513,929	2,132	-
Number of unbound binaries	1,851,730	-	-
Number of double compact objects	863	-	-
Number of mergers	0	-	-
Number of BH-NS binaries	0	3,533	-
Number of NS-BH binaries	0	269	-
Number of BH-MS binaries	1,398,490	1,441,991	29,740
Number of MS-BH binaries	0	0	0
Number of systems with semimajor axis < 3.0 AU BH-MS binaries	1,398,149	1,441,991	29,740
Number of systems with semimajor axis < 3.0 AU MS-BH binaries	0	0	-
Number of systems with orbital period < 70 days BH-MS binaries	1,397,834	1,441,624	29,660
Number of systems with orbital period < 70 days MS-BH binaries	0	0	0
Number of systems with orbital period < 30 days BH-MS binaries	-	1,440,658	29,384
Number of systems with orbital period < 30 days MS-BH binaries	-	0	0
Number of systems with semimajor axis < 0.4 AU BH-MS binaries	-	1,440,600	29,380
Number of systems with semimajor axis < 0.4 AU MS-BH binaries	-	0	0
Number of systems with orbital inclination (COSI) < 89.99° BH-MS binaries	1,539	1,656	38
Number of systems with orbital inclination (COSI) < 89.99° MS-BH binaries	0	0	0

Capture crossection from 3-body encounters

$$\widetilde{\sigma}_{\text{ej}} = \pi \left(\frac{2M_B r_{AB}}{5M_A}\right)^2 \left[-1 - \left(\frac{v_B^2 r_{AB} - 2\mu_A}{2v_B^2 r_{AB} + \mu_A}\right)^2 - \frac{v_B^2 r_{AB} + 2\mu_A}{v_B\sqrt{\mu_A r_{AB}/2}} \arctan\left(\frac{2v_B\sqrt{2\mu_A r_{AB}}}{\mu_A - 2v_B^2 r_{AB}}\right)\right. \tag{18}$$

$$\widetilde{\sigma}_{\text{cap}} \equiv \pi \left(\frac{\mu_B}{v_1^2 - v_{\text{esc}}^2}\right)^2 \left[-1 - \left(\frac{v_{\text{esc}}^2 - v_B^2}{v_1^2 - v_B^2}\right)^2 + \frac{v_{\text{esc}}^2 + v_B^2}{v_1 v_B} \arctan\left(\frac{2v_1 v_B}{v_1^2 + v_B^2}\right)\right. . \tag{19}$$

As an explanatory case, we choose to work with Starlink constellations

10 Days Starlink Positions

$\hookrightarrow$ Altitude of the of 6412 Starlink satellites with 6-second iteration intervals throughout the night observed from the Rubin Observatory in Cerro Pachón, Chile. The color scale demonstrates the azimuth of the satellite in the sky.

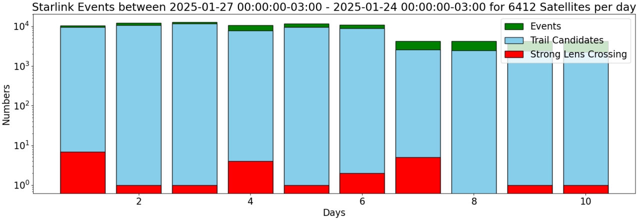

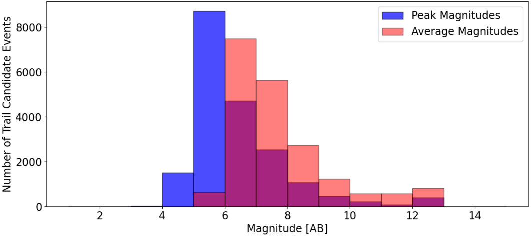

The peak magnitudes of the satellites during each trail event window and the average of these peak magnitudes for each trail event window in arcseconds.

The LSST survey is challenged by the increasing number of Sun-reflecting artificial satellites. Here we focus on the Low Earth Orbit (LEO) satellites, which are brighter due to their lower altitudes and contributing as a larger population.